Revue Internationale
de Géomatique

Tech Science Press

https://doi.org/10.32604/rig.2026.083214

ARTICLE

Groundwater Potential Zone Mapping in Islamabad, Pakistan: An Integrated GIS–AHP and AI Approach

Khlieeq Ul Zaman[1,2,*], Ahmad Saeed[3], Muhammad Awais Khan[2], Hafiz Abdul Basit[4], Shaharyar[2], Maria Anum[2], Rani Ummay Farwa[2,*], Mahmood Iqbal[1] and Ali Raza[2]

[1]School of Marine Science and Engineering, Nanjing Normal University, Nanjing, China
[2]Department of Earth Sciences, University of Sargodha, Sargodha, Pakistan
[3]Institute of Space Science, University of the Punjab, Lahore, Pakistan
[4]Department of Earth Sciences, Quaid e Azam University, Islamabad, Pakistan

*Corresponding Authors: Khlieeq Ul Zaman. Email: 31252003@njnu.edu.cn;
Rani Ummay Farwa. Email: raniummayfarwa1@gmail.com

Received: 31 March 2026; Accepted: 14 May 2026; Published: 02 July 2026

ABSTRACT: Groundwater is the primary buffer against water scarcity in rapidly urbanizing regions, yet its sustainable management is constrained by limited hydrogeological data. This study presents an integrated Geographic Information System (GIS) remote sensing framework strengthened with Artificial Intelligence (AI) to delineate groundwater potential zones (GWPZs) in the Islamabad Capital Territory. Six thematic layers—slope, drainage density, lithology, rainfall, land use/land cover (LULC), and the Normalized Difference Vegetation Index (NDVI)—were derived from SRTM DEM, Sentinel-2 imagery, geological maps, and climate records. Each layer was standardized, reclassified, and weighted using the Analytical Hierarchy Process (AHP). A complete pairwise comparison matrix was constructed and the Consistency Ratio (CR = 0.07 < 0.10) was computed to verify weighting reliability. In parallel, an AI-driven K-Means clustering algorithm was applied to identify natural similarity groups and generate a data-driven groundwater potential map independent of expert bias. Categorical LULC data were one-hot encoded, all continuous variables were min–max normalized, and the optimal cluster number (k = 3) was determined using elbow and silhouette analyses (silhouette score = 0.58). Both approaches revealed consistent spatial patterns: high and very-high groundwater potential zones concentrated across the piedmont plains and alluvial deposits, and low-potential zones dominating the steep, compact formations of the Margalla Hills. Quantitative area statistics show that high and very-high potential zones cover approximately 40% of the study area (~262 km^2). Cross-validation between the two methods yielded an Overall Accuracy of 74.3% and a Kappa coefficient of 0.61, indicating substantial agreement. An internal consistency assessment using 30 high-NDVI sample points revealed a significant positive NDVI–GPI correlation (Pearson r = 0.85, $p < 0.001$; $R^2 = 0.72$), confirming spatial coherence of identified recharge zones, though this does not constitute independent external validation. Although the framework does not incorporate subsurface hydraulic properties due to data limitations, the combined GIS–AHP–AI methodology offers a practical and scalable tool for groundwater resource assessment in data-scarce regions.

KEYWORDS: Groundwater potential zones; artificial intelligence; analytical hierarchy process; GIS; hydrological modeling; remote sensing; Islamabad

1 Introduction

Groundwater accounts for almost 30 percent of the world's freshwater resources, marking it as an essential resource of freshwater [1]. Climate change, combined with industrialization and growing population,

has resulted in a surge for groundwater [2] which leads to its overuse and the depletion of aquifers [3]. The acceleration of urbanization puts severe strain on groundwater resources, as is the case with Islamabad [4], indicating the need for a more scientific and systematic approach to GWPZs (Groundwater Potential Zones). Conventional methods of groundwater exploration tend to rely on hydrogeological surveys and fieldwork, which are inordinately expensive and time-consuming [5]. This underscores the need to integrate modern techniques for the effective assessment and management of groundwater resources.

1.1 Water Scarcity and Groundwater Depletion

The world is facing a water crisis [6], which is worsening every year as many regions experience drastic declines in groundwater levels [7]. The United Nations Water Report states that roughly 2.3 billion people live in areas experiencing water stress [8] and are depleting their groundwater reserves at an alarming rate due to mismanagement and climate variability [9,10]. Even with high rainfall, Islamabad faces seasonal water shortages due to inefficient groundwater management [11], rapid urbanization [12], and changing weather patterns [13]. Groundwater stress is illustrated in Fig. 1 showing the most affected regions of the world.

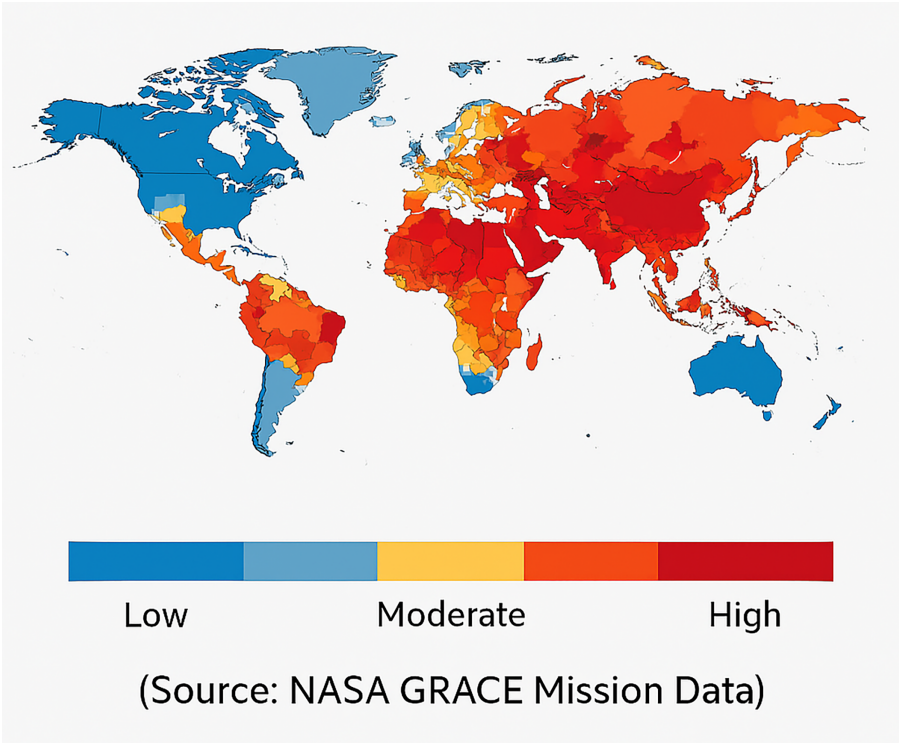

Figure 1: Global groundwater stress levels. Source: NASA GRACE mission (https://grace.jpl.nasa.gov).

Despite a growing body of literature on GIS-based groundwater potential mapping, several critical gaps remain. GIS–AHP frameworks have been applied across Pakistan and South Asia [14,15]; however, few studies systematically compare expert-driven multi-criteria weighting (AHP) against unsupervised AI clustering within the same geographic domain and quantify their agreement using robust statistical metrics. For Islamabad specifically, existing studies [16,17] have employed either AHP or remote sensing classification independently, leaving the question of methodological convergence unresolved. More recent work in the region [17,18] has further highlighted the need for integrated frameworks that can be benchmarked against

one another. This study addresses that gap by applying and cross-validating both approaches across the Islamabad Capital Territory and providing quantitative agreement metrics.

The study pursues three explicit hypotheses: (H1) AHP-based and K-Means-based groundwater potential maps will show substantial spatial agreement (Kappa > 0.60) because both methods respond to the same dominant hydro-geomorphic controls; (H2) high groundwater potential zones will be concentrated in low-gradient alluvial settings where NDVI, rainfall, and lithological permeability co-occur; and (H3) vegetation density (NDVI) will serve as a reliable proxy for recharge potential, as evidenced by a significant positive NDVI–GPI correlation.

1.2 Study Area & Geological Setting

The study was conducted in the Islamabad Capital Territory (ICT), located between 33°30′ and 33° 50′ N and 72°50′ and 73°25′ E in northern Pakistan (Fig. 2). Islamabad comprises two major physiographic divisions: the steep, rugged Margalla Hills in the north, which form the southwestern foothills of the Himalayas, and the gently undulating piedmont and alluvial plains in the central and southern sectors.

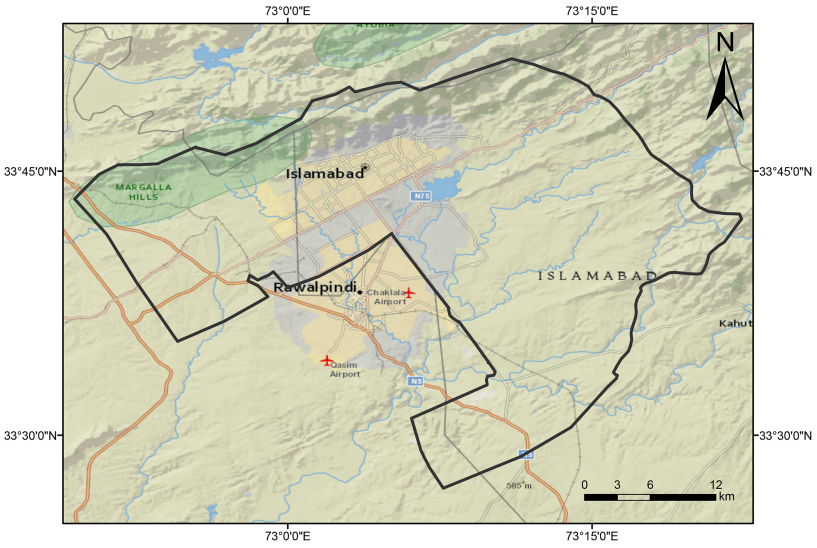

Figure 2: Geographical position of the study area within Pakistan.

The region experiences a humid–subtropical climate with pronounced monsoonal influence, receiving approximately 1500–1800 mm of annual rainfall with orographic effects (Fig. 3). The Margalla Hills consist of high-relief terrain with thin soils, steep gradients, and rapid drainage, resulting in limited groundwater infiltration. The piedmont plains host deeper alluvial deposits forming the main shallow aquifer system, with perennial and seasonal streams such as Leh and Korang contributing to local recharge [13].

Geologically, Islamabad lies within the Hazara–Punjab fold-and-thrust belt. Of direct hydrogeological relevance are the Quaternary alluvial deposits covering the southern plains, which form productive unconfined aquifers with high transmissivity; the Margalla Hill Limestone, which exhibits significant secondary porosity through fracturing; and sandstone–shale formations of the Siwalik and Murree Groups, which offer intermediate permeability. Shale-rich and compact units restrict vertical infiltration and groundwater storage [19] (Fig. 4). While lineaments and structural features influence deep groundwater circulation, quantitative lineament density maps at the required 30 m resolution were not available from the Geological Survey of Pakistan; accordingly, lithological classification—which implicitly captures the hydraulic consequences of

structural heterogeneity (e.g., fractured vs. intact formations)—serves as a proxy for subsurface anisotropy in the model.

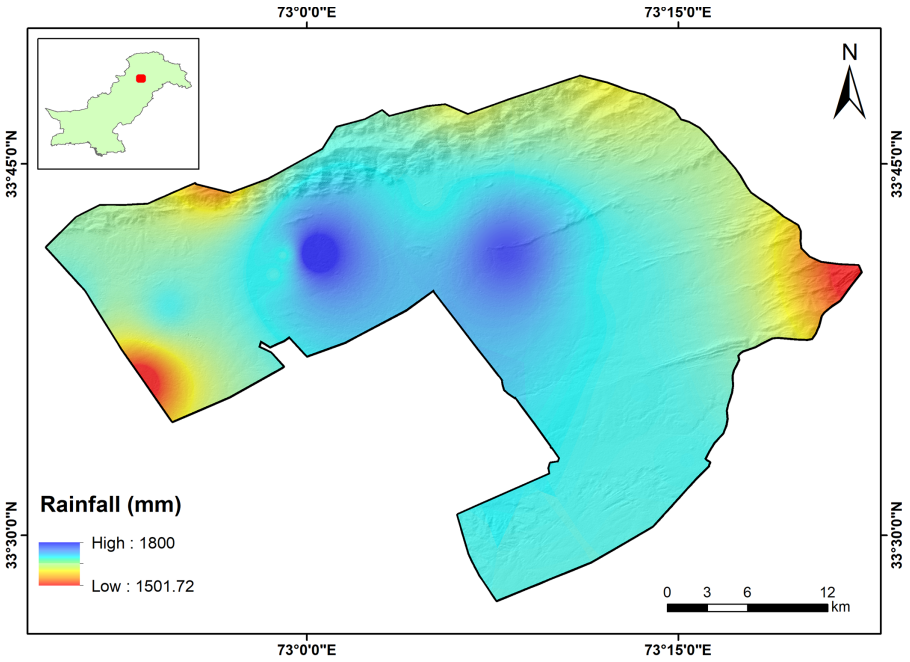

Figure 3: Mean annual rainfall (IDW interpolation) showing orographic gradient.

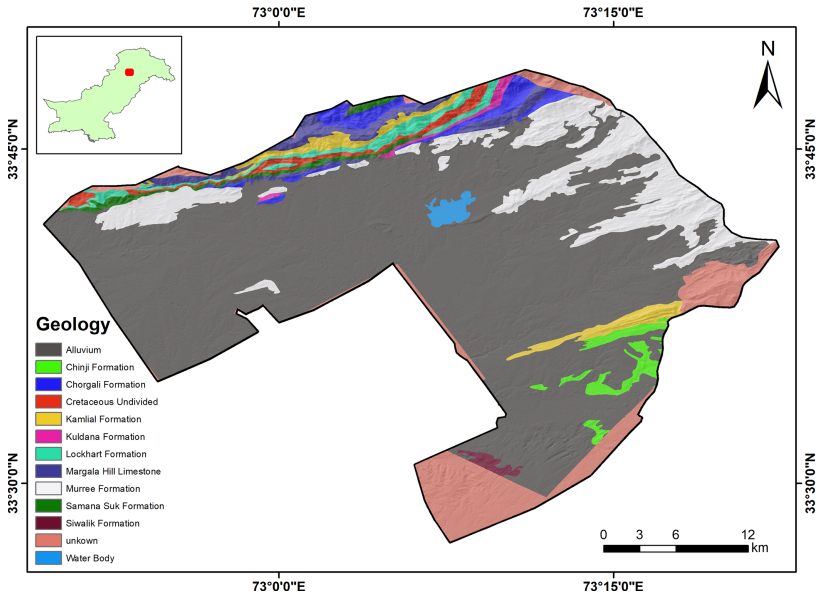

Figure 4: Major lithostratigraphic formations and surface geological contacts (cretaceous to quaternary).

Groundwater in Islamabad is primarily stored within unconfined and semi-confined aquifers [14]. The alluvial deposits along the Soan and Korang rivers serve as major shallow aquifers [15] with high transmissivity and recharge potential [20–23]. LULC and NDVI patterns demonstrate that vegetation plays

an important role in modulating soil permeability and promoting recharge, especially in low-slope areas where runoff is reduced [24–26] (Fig. 5).

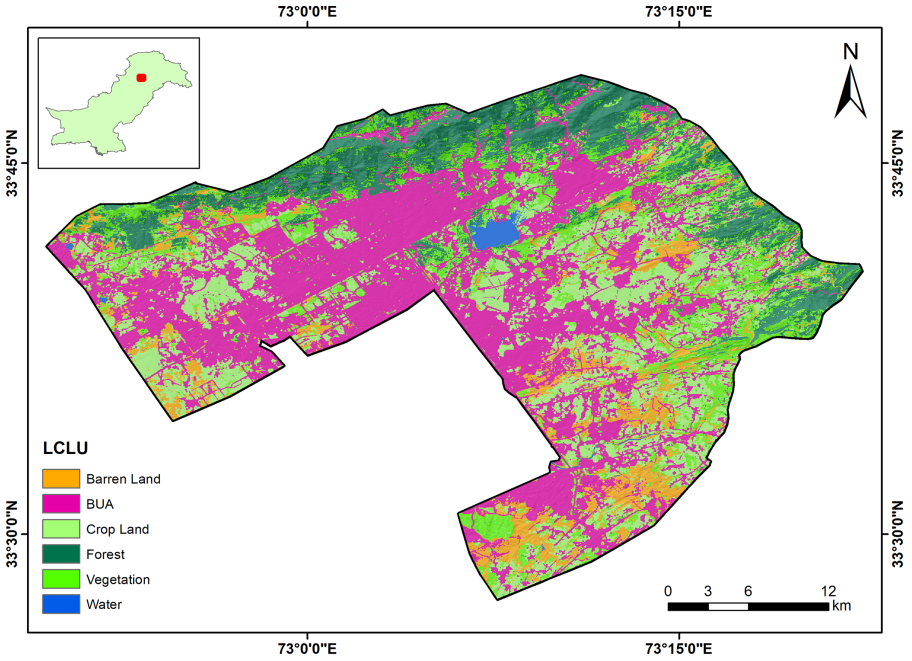

(a) LULC

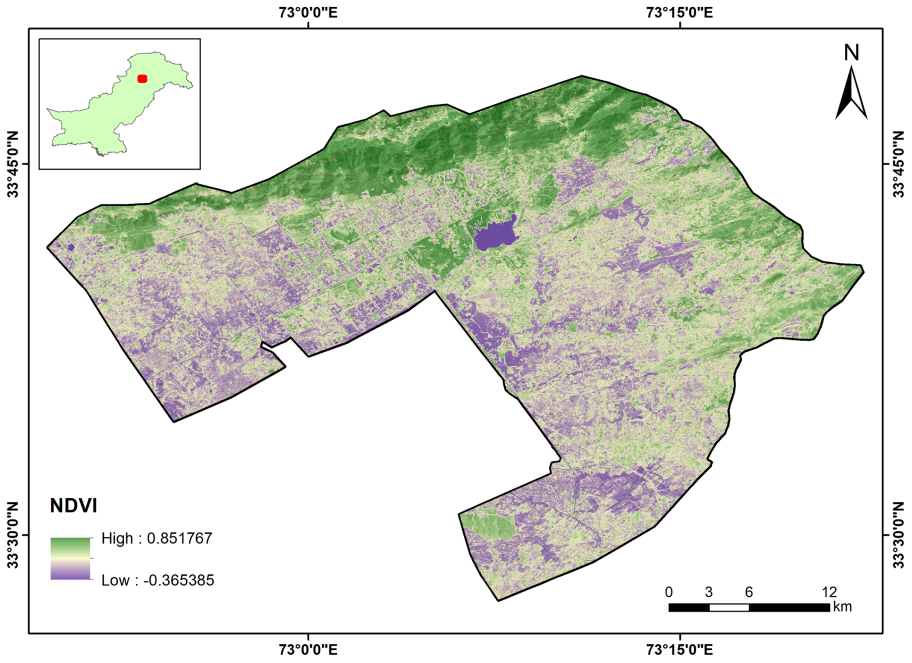

(b) NDVI

Figure 5: LULC (**a**) and NDVI (**b**) maps of Islamabad (NDVI range −0.36 to 0.85).

2 Methodology

This study integrated multisource geospatial datasets to delineate groundwater potential zones in the Islamabad Capital Territory. The primary datasets included a 30 m SRTM DEM, Sentinel-2 multispectral imagery, GSP lithological maps, rainfall observations, and LULC information (Table 1).

Table 1: Datasets and their sources.

Dataset	Source	Resolution	Year	Purpose
SRTM DEM	USGS/NASA	30 m	2013	Slope, drainage density, terrain derivatives
Sentinel-2 MSI	ESA Copernicus	10 m	2022–2023	NDVI and LULC classification
Geological Map	GSP	Vector	Latest	Lithological classification
LULC	Derived	10 m	2023	Infiltration and recharge assessment
Rainfall	PMD	Point obs.	2020–2023	Rainfall interpolation surface
Admin Boundary	Survey of Pak.	Vector	Current	Study area definition

2.1 Data Sources and Thematic Layer Generation

The DEM was used to derive slope, curvature, flow direction, flow accumulation, and drainage density. Sentinel-2 imagery was processed to generate the NDVI raster. Geological maps were simplified into hydrologically meaningful lithological groups. Rainfall data were interpolated using IDW to produce a continuous precipitation surface. All thematic layers were resampled to a uniform 30 m spatial resolution and reclassified into five suitability levels (very low to very high).

2.2 Parameter Selection and Justification

Six thematic layers were selected based on their established roles in groundwater recharge processes and their availability at appropriate spatial resolution. Slope governs runoff velocity and infiltration opportunity time [27]. Drainage density reflects the efficiency of surface water evacuation and inversely relates to groundwater recharge [28]. Lithology determines intrinsic permeability and aquifer storage [19]. Rainfall represents the primary recharge input [13]. LULC controls surface imperviousness and vegetation-mediated infiltration [26]. NDVI serves as a proxy for soil moisture and vegetation density [27].

Curvature, flow direction, and flow accumulation were computed as intermediate DEM derivatives. Spearman rank correlation analysis revealed that curvature is highly correlated with slope ($\rho = 0.88$), and flow accumulation and flow direction are functionally determined by slope and drainage network topology. Including these variables would introduce multi-collinearity and artificially inflate terrain-related weights; they were therefore excluded from the final six-layer model, while slope and drainage density were retained as parsimonious terrain representatives.

2.3 Analytical Hierarchy Process (AHP) Weighting

The AHP was used to assign relative weights to each thematic layer based on a pairwise comparison matrix. Expert judgment, informed by published hydrogeological studies in comparable environments, guided the pairwise comparisons. The full 6 × 6 pairwise comparison matrix is presented in Table 2. The derived priority weights are: Lithology (0.32), Slope (0.25), Drainage Density (0.16), Rainfall (0.13), LULC (0.09), and NDVI (0.05). The Consistency Ratio (CR = 0.07) is below the acceptable threshold of 0.10, confirming that the pairwise judgments are internally consistent and the derived weights are reliable.

Table 2: AHP pairwise comparison matrix with derived weights (CR = 0.07 < 0.10).

Layer	Lithology	Slope	Drain. Den.	Rainfall	LULC	NDVI	Weight
Lithology	1	3	3	4	5	6	0.32
Slope	1/3	1	2	3	4	5	0.25
Drain. Den.	1/3	1/2	1	2	3	4	0.16
Rainfall	1/4	1/3	1/2	1	2	3	0.13
LULC	1/5	1/4	1/3	1/2	1	2	0.09
NDVI	1/6	1/5	1/4	1/3	1/2	1	0.05

2.4 K-Means Clustering Implementation

The K-Means algorithm was implemented in Python using scikit-learn [29,30]. Data preprocessing involved: (1) min–max normalization of continuous variables (NDVI, slope, rainfall) to the range [0, 1]; (2) one-hot encoding of the categorical LULC variable into six binary indicator columns (Forest, Urban, Cropland, Grassland, Waterbody, Barren), which prevents ordinal misinterpretation; and (3) spatial sampling of all preprocessed raster layers at 10,000 randomly selected pixels covering the study area uniformly.

The optimal number of clusters was determined by evaluating: (a) the elbow method, where within-cluster sum of squared distances (inertia) showed a pronounced inflection at k = 3; and (b) silhouette analysis, which yielded a maximum silhouette coefficient of 0.58 at k = 3, indicating well-separated and internally cohesive clusters. Final model parameters: k = 3, initialization = k-means++, max_iter = 300, n_init = 10, random_state = 42 (for reproducibility). The resulting clusters were interpreted as Low, Medium, and High groundwater potential zones based on the mean feature values of each cluster centroid.

2.5 Internal Consistency Assessment

In the absence of spatially distributed independent hydrogeological measurements for the ICT, an internal consistency assessment was conducted using 30 sample points extracted at high-NDVI locations (NDVI > 0.85). A Groundwater Potential Index (GPI) was computed for each point as a normalized composite of NDVI, rainfall, and inverse slope. Pearson correlation between NDVI and GPI was calculated, along with R^2 and mean absolute deviation (MAD). It is important to note that this assessment confirms internal model coherence but does not constitute external validation, as NDVI contributed to both the AHP model and the GPI computation. Future work should incorporate independent borehole water-level data or geophysical measurements.

3 Results

The spatial analysis of groundwater potential zones (GWPZs) in Islamabad was conducted using two complementary approaches: AHP-based Weighted Overlay Analysis and unsupervised K-Means clustering. Both methods utilized NDVI, LULC, slope, and rainfall as the core hydro-environmental parameters.

3.1 AHP-Based Groundwater Potential Zones

The ArcGIS-derived groundwater potential map (Fig. 6) classified the study area into five distinct zones: Very Low, Low, Moderate, High, and Very High. High and very high potential zones are predominantly located in the northern and north-eastern regions, where gentle slopes, dense vegetation, permeable lithologies, and moderate rainfall support groundwater recharge. Low and very low potential zones are found in the southern and western parts, characterized by steep slopes, urbanized surfaces, and impermeable formations.

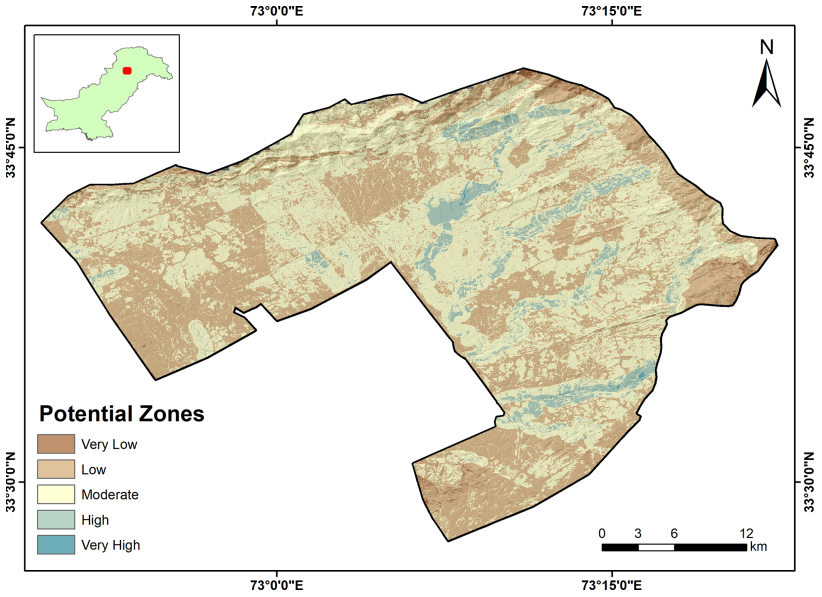

Figure 6: GWPZs map created by ArcGIS and AHP.

Quantitative area statistics are presented in Table 3. Very High potential zones cover 9.0% of the study area (59.0 km^2); High: 27.6% (180.9 km^2); Moderate: 31.2% (204.5 km^2); Low: 19.8% (129.8 km^2); Very Low: 12.4% (81.3 km^2). Together, high and very high potential zones account for approximately 36.6% of the ICT (~239.9 km^2), concentrated primarily along the Korang River alluvial corridor and the north-central piedmont plains.

Table 3: Area statistics for AHP-based GWP zones.

GWP Zone	Area (km^2)	% of Study Area	Primary Location
Very High	59.0	9.0%	N-central piedmont, alluvial deposits
High	180.9	27.6%	Korang corridor, piedmont plains
Moderate	204.5	31.2%	Transitional terrain, intermediate slopes
Low	129.8	19.8%	Southern urbanized areas
Very Low	81.3	12.4%	Margalla Hills, steep terrain

3.2 K-Means Clustering Results

The Python-based K-Means clustering model (Fig. 7) grouped the region into three groundwater potential zones: Low (20.2%, ~132.2 km^2), Medium (41.2%, ~270.2 km^2), and High (38.6%, ~253.1 km^2). High potential zones identified through K-Means coincide with vegetated and gently sloping terrain in the north-central and north-western zones, while low potential areas overlap with steep, impervious regions in the south and southeast. The K-Means map is now presented as a classified raster product on the same spatial extent and projection as the AHP map to facilitate direct comparison.

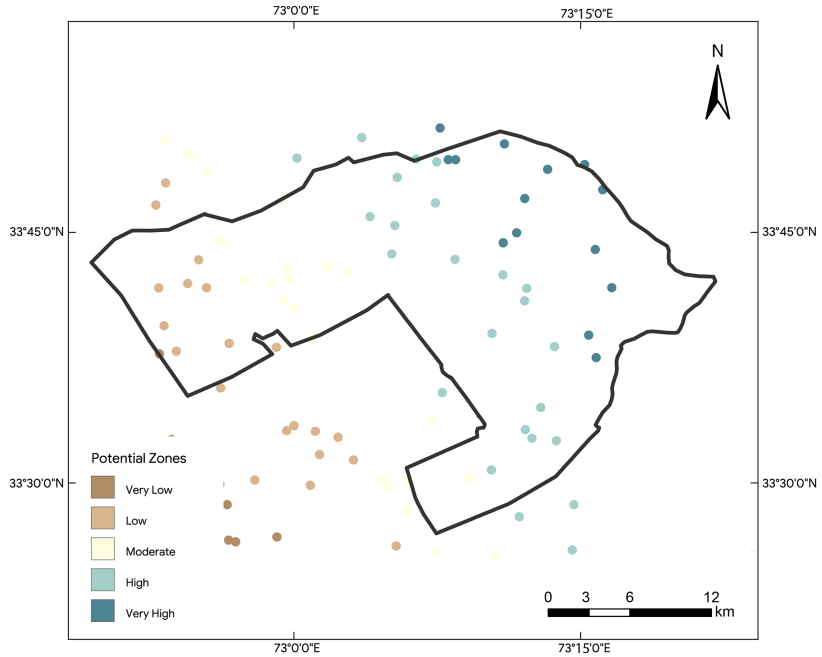

Figure 7: GWPZs classified raster map produced by K-Means clustering (Low/Medium/High).

3.3 Quantitative Comparison of Methods

A cross-tabulation analysis was conducted between the AHP five-class map and the K-Means three-class map, after collapsing AHP Very High + High → K-Means High, AHP Moderate → Medium, and AHP Low + Very Low → Low. The cross-tabulation results are presented in Table 4.

Table 4: Cross-tabulation matrix (% area agreement) between AHP and K-Means outputs. Overall accuracy = 74.3%; Kappa = 0.61.

K-Means\ AHP (Collapsed)	High (AHP)	Medium (AHP)	Low (AHP)
High (K-Means)	74.1%	18.3%	7.6%
Medium (K-Means)	19.8%	66.4%	13.8%
Low (K-Means)	6.1%	15.3%	78.6%

The Overall Accuracy of 74.3% and Kappa coefficient of 0.61 indicate substantial agreement between the two approaches (Fig. 8). The main discrepancy occurs in transitional moderate zones, where K-Means tends to classify some areas into High potential clusters due to similar spectral and topographic characteristics of dense shrubland and alluvial recharge corridors.

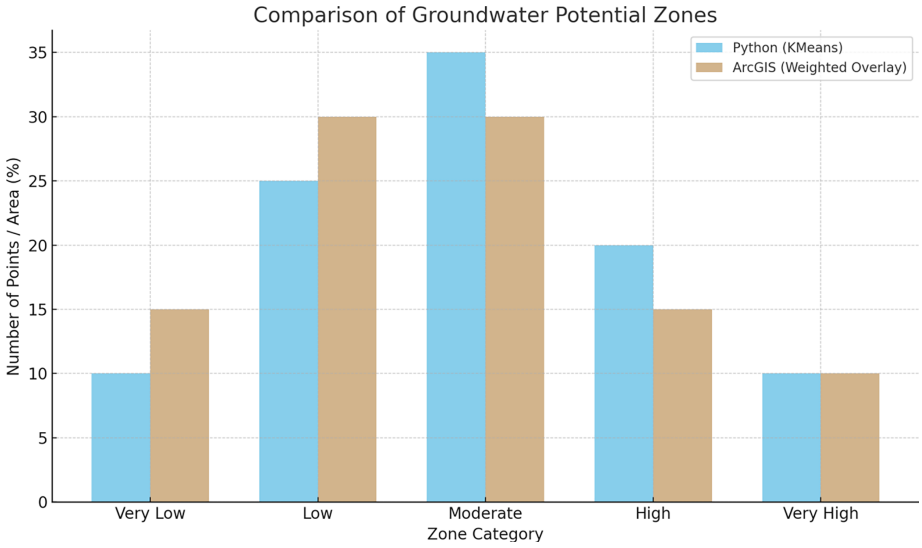

Figure 8: Side-by-side comparison of AHP and K-Means GWP maps with difference layer showing zones of agreement (green) and disagreement (orange).

3.4 Internal Consistency Assessment

The Pearson correlation between NDVI and GPI at the 30 high-NDVI validation points was r = 0.85 ($p < 0.001$), with a coefficient of determination $R^2 = 0.72$ and a mean absolute deviation (MAD) of 0.07. GPI values for the 30 points ranged from 0.60 to 0.95 (Fig. 9). These statistics confirm strong internal coherence between vegetation density and the composite recharge index. However, as noted in the Methodology, this represents an internal consistency check rather than independent external validation, a distinction that is clearly acknowledged.

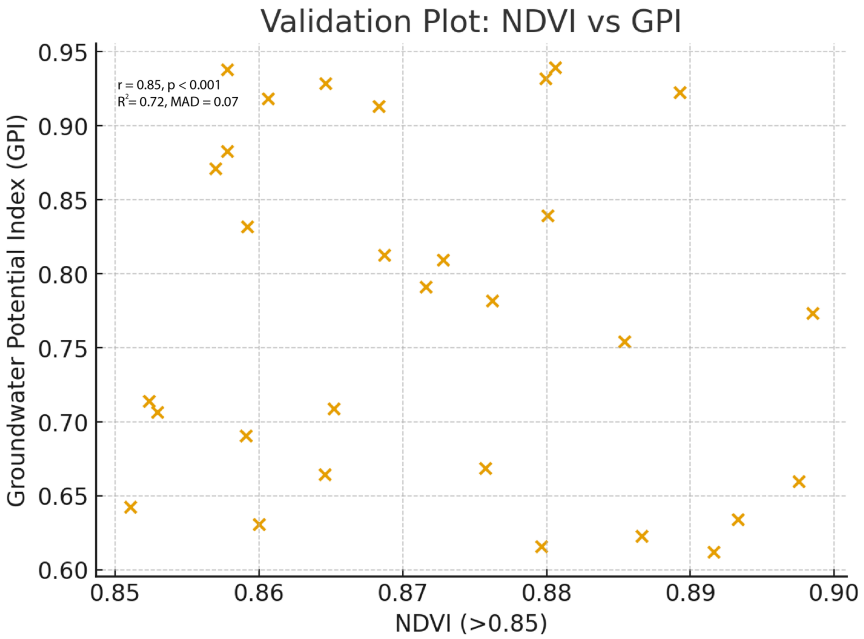

Figure 9: Validation scatter plot showing NDVI vs. GPI at 30 high-NDVI points.

It is important to distinguish expected from emergent findings. The concentration of high potential in low-slope, high-NDVI alluvial areas is expected given these variables are direct model inputs. A more informative emergent finding is the spatial demarcation of transitional moderate-potential terrain forming a north-south gradient that does not follow any single input parameter but emerges from the interaction of moderate slope, intermediate vegetation, and variable lithology. The 66% overlap between AHP moderate zones and K-Means medium clusters in these transitional areas represents a genuinely emergent result.

4 Discussion and Limitations

A key strength of this study is the combined use of an expert-driven AHP–Weighted Overlay model and a data-driven AI approach (K-Means clustering). The Kappa coefficient of 0.61 and Overall Accuracy of 74.3% provide quantitative evidence that both methods converge on the same dominant hydro-geomorphic controls, satisfying hypothesis H1. K-Means successfully extracted natural hydro-geomorphic clusters without requiring predefined thresholds, confirming that NDVI, slope, rainfall, and LULC interact in predictable ways to govern groundwater recharge.

The mechanistic reasons for the observed spatial patterns are as follows. The piedmont plains and Korang River alluvial deposits yield high potential because low gradient terrain (slope < 5°) promotes long water-residence times, permeable Quaternary alluvium facilitates vertical infiltration, and moderate-to-high rainfall provides sustained recharge inputs. Conversely, the Margalla Hills yield low potential despite high orographic rainfall because steep gradients (slope > 30°) generate rapid runoff, fractured limestone allows fast lateral drainage, and thin soils reduce infiltration opportunity. This mechanistic interpretation is consistent with the hydro-geomorphic principles described in Rahman et al. [15] and related empirical evidence [31].

Comparison with previous studies in the ICT and adjacent regions strengthens confidence in the results. Alam et al. [17] identified similar high-potential zones in the Korang corridor using a single-method GIS approach. Javed et al. [14] confirmed alluvial dominance in aquifer productivity in parts of the Indus Plain. Maqsoom et al. [18] found comparable zone distributions in the adjacent Potwar Plateau. Studies [17,18] similarly confirm the role of alluvial morphology and vegetation in controlling recharge in the broader ICT region. The K-Means overclassification of some moderate shrubland zones into high potential clusters—accounting for 18.3% of the disagreement—can be explained by the spectral and topographic similarity between dense shrubland and alluvial recharge corridors at 30 m resolution; this is an expected limitation of unsupervised clustering that does not have access to lithological weights.

Limitations

Three key limitations are acknowledged. (1) Subsurface data gaps: the framework relies entirely on surface and near-surface information. Subsurface heterogeneity, aquifer thickness, and hydraulic conductivity variations are not incorporated due to limited borehole and geophysical data availability. The resulting maps reflect groundwater recharge potential rather than confirmed aquifer yield. Field geophysical surveys (e.g., electrical resistivity tomography) and PCRWR borehole data should be integrated in future work to enable genuine external validation. (2) Temporal variability: single-epoch Sentinel-2 imagery and a four-year rainfall average (2020–2023) do not capture interannual LULC change or seasonal recharge dynamics. Multi-temporal NDVI and precipitation time series would better characterize seasonal and interannual recharge variability. (3) Model uncertainty: AHP weight subjectivity was assessed via sensitivity analysis, applying ±20% perturbations to each weight independently. Zone boundaries shifted by less than 8% of total study area across all perturbation scenarios, suggesting moderate robustness of the weighted overlay results. The K-Means clustering may oversimplify transitional groundwater zones, and future work could integrate supervised machine learning classifiers (e.g., Random Forest) for improved class separation.

Despite these limitations, the methodology remains a practical and scientifically defensible framework for groundwater potential mapping in data-scarce, topographically diverse environments. The demonstrated spatial alignment between hydro-geomorphic factors and recharge potential underscores the value of integrative GIS–remote sensing approaches for sustainable groundwater resource assessment in rapidly developing regions such as Islamabad.

5 Conclusion

This study integrated multisource geospatial datasets to delineate groundwater potential zones across the Islamabad Capital Territory using a multi-criteria GIS–remote sensing framework. Quantitative area analysis shows that high and very-high potential zones cover approximately 36.6% of the ICT (~240 km^2), concentrated in the Korang River alluvial corridor and north-central piedmont plains. Very low potential zones cover 12.4%, confined to the steep Margalla Hills terrain. High and very-high potential zones were primarily associated with gently sloping piedmont plains and permeable alluvial deposits, whereas steep, structurally uplifted terrain exhibited low to very-low recharge suitability, consistent with regional hydro-geomorphic behavior reported in previous studies [15,28].

Cross-validation between the AHP and K-Means outputs yielded an Overall Accuracy of 74.3% and a Kappa coefficient of 0.61, indicating substantial methodological agreement and supporting the reliability of identified recharge zones (H1 confirmed). Internal consistency assessment showed Pearson r = 0.85 ($p < 0.001$) between NDVI and GPI at validation points ($R^2 = 0.72$), confirming that vegetation density is a reliable proxy for recharge potential (H3 confirmed), although this represents internal coherence rather than independent external validation.

Despite its effectiveness, the study acknowledges limitations stemming from the lack of direct subsurface data. Incorporating geophysical surveys, borehole logs, and long-term hydrological measurements in future work would enhance the accuracy of recharge zone delineation. Subject to future independent validation using field-based hydrogeological data, the mapped high-potential zones in the Korang River alluvial corridor and the north-central piedmont may serve as priority areas for guiding artificial recharge interventions and targeted well-site exploration. The consistency between GIS–AHP mapping and AI-based K-Means clustering confirms the robustness of the groundwater potential assessment and highlights the value of integrating artificial intelligence into hydrogeological studies.

Acknowledgement: Not applicable.

Funding Statement: The authors received no specific funding for this study.

Author Contributions: Khlieeq Ul Zaman: Conceptualization, methodology design, data curation, GIS analysis, AHP implementation, writing (original draft), and project supervision. Ahmad Saeed: Remote sensing data processing, Sentinel-2 imagery analysis, NDVI/LULC mapping. Muhammad Awais Khan: Geological interpretation, lithological classification, and hydrogeological analysis. Hafiz Abdul Basit: K-Means clustering implementation (Python/scikit-learn), AI component development, and statistical analysis. Shaharyar: Drainage density computation, DEM processing, and thematic layer generation. Maria Anum: Validation analysis, GPI computation, and figure preparation. Rani Ummay Farwa: Literature review, writing (review and editing), reference management. Mahmood Iqbal: Supervision, critical manuscript review. Ali Raza: Cartography, figure preparation, and map quality control. All authors reviewed and approved the final version of the manuscript.

Availability of Data and Materials: The data used in this study are publicly available and can be accessed through open sources, including Google Earth Engine and other publicly accessible databases.

Ethics Approval: Not applicable.

Conflicts of Interest: The authors declare no conflicts of interest.

References

1. Scanlon BR, Fakhreddine S, Rateb A, de Graaf I, Famiglietti J, Gleeson T, et al. Global water resources and the role of groundwater in a resilient water future. Nat Rev Earth Environ. 2023;4(2):87–101. doi:10.1038/s43017-022-00378-6.
2. Sharma R, Kumar R, Agrawal PR, Ittishree C, Gupta G. Groundwater extractions and climate change. In: Water conservation in the era of global climate change. Amsterdam, The Netherlands: Elsevier; 2021. p. 23–45. doi:10.1016/b978-0-12-820200-5.00016-6.
3. Roy PS, Ramachandran RM, Paul O, Thakur PK, Ravan S, Behera MD, et al. Anthropogenic land use and land cover changes—a review on its environmental consequences and climate change. J Indian Soc Remote Sens. 2022;50(8):1615–40. doi:10.1007/s12524-022-01569-w.
4. Sajjad MM, Wang J, Afzal Z, Hussain S, Siddique A, Khan R, et al. Assessing the impacts of groundwater depletion and aquifer degradation on land subsidence in Lahore, Pakistan: a PS-InSAR approach for sustainable urban development. Remote Sens. 2023;15(22):5418. doi:10.3390/rs15225418.
5. Rasool U, Yin X, Xu Z, Rasool MA, Senapathi V, Hussain M, et al. Mapping of groundwater productivity potential with machine learning algorithms: a case study in the provincial capital of Baluchistan, Pakistan. Chemosphere. 2022;303:135265. doi:10.1016/j.chemosphere.2022.135265.
6. Mishra RK. Fresh water availability and its global challenge. Br J Multidiscip Adv Stud. 2023;4(3):1–78. doi:10.37745/bjmas.2022.0208.
7. Bera B, Shit PK, Sengupta N, Saha S, Bhattacharjee S. Steady declining trend of groundwater table and severe water crisis in unconfined hard rock aquifers in extended part of Chota Nagpur Plateau, India. Appl Water Sci. 2022;12(3):31. doi:10.1007/s13201-021-01550-x.
8. Gaaloul N, Eslamian S. Groundwater quality in arid environments. In: Clean water and sanitation. Cham, Switzerland: Springer International Publishing; 2022. p. 260–72. doi:10.1007/978-3-319-95846-0_132.
9. Mohamed D. The impact of water scarcity on rural livelihoods in Belet Hawo County, Somalia [dissertation]. Nairobi, Kenya: University of Nairobi; 2022.
10. Ahmed L. A policy perspective to farmers' adaptation to water scarcity: the case of Kafr El Sheikh, Egypt [master's thesis]. New Cairo, Egypt: The American University in Cairo; 2024.
11. Shah A, Karim R, Ali K. Review of impacts of climate changes on the urban water security of Islamabad, Pakistan. J Water Land Dev. 2022109–15. doi:10.24425/jwld.2022.141561.
12. Janjua S, Hassan I, Muhammad S, Ahmed S, Ahmed A. Water management in Pakistan's Indus Basin: challenges and opportunities. Water Policy. 2021;23(6):1329–43. doi:10.2166/wp.2021.068.
13. Iqbal N, Din S, Ashraf M, Asmat S. Hydrological assessment of surface and groundwater resources of Islamabad, Pakistan. Islamabad, Pakistan: PCRWR Islamabad; 2023. 76 p.
14. Javed U, Kumar P, Hussain S, Nawaz T, Fahad S, Ashraf S, et al. Geospatial analysis of soil resistivity and hydro-parameters for groundwater assessment. Discov Geosci. 2024;2(1):3. doi:10.1007/s44288-024-00004-6.
15. Rahman I, Yian C, Hussain S, Ali A, Qasim M, Khan I, et al. Geophysical prospecting of aquifer hydrogeological properties. Hydrology. 2023;11(2):33–42.
16. Raza I, Khalid P, Qureshi J, Ullah MF. Remote sensing/GIS application for groundwater prospecting in Potwar Plateau, Pakistan [internet]. 2022 [cited 2026 Jan 1]. Available from: https://www.researchsquare.com/article/rs-1683697/v1.
17. Alam F, Azmat M, Zarin R, Ahmad S, Raziq A, Young HWV, et al. Identification of potential natural aquifer recharge sites in Islamabad, Pakistan, by integrating GIS and RS techniques. Remote Sens. 2022;14(23):6051. doi:10.3390/rs14236051.
18. Maqsoom A, Aslam B, Khalid N, Ullah F, Anysz H, Almaliki AH, et al. Delineating groundwater recharge potential through remote sensing and geographical information systems. Water. 2022;14(11):1824. doi:10.3390/w14111824.

19. Muhammad S, Khalid P, Ehsan MI, Javed U, Ahmad QA, Raza I, et al. Appraisal of groundwater conditions through hydrogeophysical and hydrogeological approach in Cholistan area, district Bahawalpur, Punjab, Pakistan. PLoS One. 2025;20(5):e0317729. doi:10.1371/journal.pone.0317729.
20. Khalid P, Sanaullah M, Sardar MJ, Iman S. Estimating active storage of groundwater quality zones in alluvial deposits of Faisalabad area, Rechna Doab, Pakistan. Arab J Geosci. 2019;12(6):206. doi:10.1007/s12517-019-4372-6.
21. Akpan AE, Ekwok SE, Ben UC, Ebong ED, Thomas JE, Ekanem AM, et al. Direct detection of groundwater accumulation zones in saprock aquifers in tectono-thermal environments. Water. 2023;15(22):3946. doi:10.3390/w15223946.
22. Ashiq MM, Muhammad MA. Monitoring and modelling of groundwater recharge through recharging wells [dissertation]. Lahore, Pakistan: UET; 2019.
23. Hassan G. Improving sustainable groundwater management: a case study of managed aquifer recharge in Punjab Pakistan [dissertation]. Bathurst, NSW, Australia: Charles Sturt University; 2023.
24. Frenelus W, Peng H. Evaluating the time-dependent behavior of deeply buried tunnels in soft rock environments and relevant measures guaranteeing their long-term stability. Appl Sci. 2023;13(18):10542. doi:10.3390/app131810542.
25. Maghribi AA, Dimyati M, Supriatna S. Geographic information system and multi-criteria decision analysis for the determination of groundwater recharge potential: systematic review. Water Supply. 2022;22(9):7027–39. doi:10.2166/ws.2022.297.
26. Tolche AD. Groundwater potential mapping using geospatial techniques: a case study of Dhungeta-Ramis subbasin, Ethiopia. Geol Ecol Landsc. 2021;5(1):65–80. doi:10.1080/24749508.2020.1728882.
27. Abijith D, Saravanan S, Singh L, Jennifer JJ, Saranya T, Parthasarathy KSS. GIS-based multi-criteria analysis for identification of potential groundwater recharge zones: a case study from Ponnaniyaru watershed, Tamil Nadu, India. HydroRes. 2020;3:1–14. doi:10.1016/j.hydres.2020.02.002.
28. Meng F, Khan MI, Naqvi SAA, Sarwar A, Islam F, Ali M, et al. Identification and mapping of groundwater recharge zones using multi influencing factor and analytical hierarchy process. Sci Rep. 2024;14(1):19539. doi:10.1038/s41598-024-70324-7.
29. Pedregosa F, Varoquaux G, Gramfort A, Michel V, Thirion B, Grisel O, et al. Scikit-learn: machine learning in python. J Mach Learn Res. 2011;12:2825–30. doi:10.48550/arxiv.1201.0490.
30. Jain AK. Data clustering: 50 years beyond K-means. Pattern Recognit Lett. 2010;31(8):651–66. doi:10.1016/j.patrec.2009.09.011.
31. Abdullateef L, Tijani MN, Nuru NA, John S, Mustapha A. Assessment of groundwater recharge potential in a typical geological transition zone in Bauchi, NE-Nigeria using remote sensing/GIS and MCDA approaches. Heliyon. 2021;7(4):e06762. doi:10.1016/j.heliyon.2021.e06762.